

Biomedical Applications of Titanium and Aluminium-based High Entropy Alloys

Vrushali Patil^{1*}, Santosh Balivada², Sathvik Appagana³

¹National Institute of Pharmaceutical Education and Research, S.A.S. Nagar, India

²Center of Excellence-Additive Manufacturing, AMTZ, Vishakhapatnam, Andhra Pradesh, India

³Gandhi Institute of Technology and Management (GITAM) University, India

Received: 18th February, 2022; Accepted: 20nd March, 2022; Available Online: 22nd March, 2022

ABSTRACT

High entropy alloys are a subclass of metallic biomaterials whose biomedical applications are vigorously explored in recent times due to their excellent mechanical properties and biocompatibility. Most of the current biomaterials are a tradeoff between biocompatibility and mechanical properties or tribological properties. For overcoming this problem, high entropy alloys are introduced into the field of biomaterials. They arise because of development in modern technologies especially, processing technologies such as Arc melting, RF magnetron sputtering, powder metallurgy, vacuum arc melting, cold rolling, selective laser sintering, etc. The gross resultant properties of high entropy alloys are a function of the composition of the metals used, processing methods, compatibility between the alloys, and many other parameters. Hence, in the following review the factors that affect the overall properties of high entropy alloys that are made up of titanium and aluminum along with their mechanical properties, tribological properties are discussed for their application in many load-bearing areas in a human body.

Keywords: Aluminum alloys, Biomedical Applications, High Entropy Alloys, Orthopedic applications, Titanium alloys.
International Journal of Health Technology (2022)

How to cite this article: Patil V, Balivada S, Appagana S. Biomedical Applications of Titanium and Aluminium-based High Entropy Alloys. International Journal of Health Technology. 2022;1(1):40-48.

Source of support: Nil.

Conflict of interest: None

INTRODUCTION

Biomaterials are materials that aid in the temporary or permanent replacement of damaged tissues or an injured organ.¹ They're employed in everything from scaffolding cells and tissues to joint replacements in the biomedical field. They are classified as synthetic or natural biomaterials depending on the material from which they are made. Metallic, ceramic, Polymeric and other composite biomaterials are examples of synthetic biomaterials. Natural biomaterials include natural silk, chitosan, and collagen.² However synthetic biomaterials gained popularity because of their simplicity and their ease of handling. The choice of material depends upon the location of the application because the biomechanics of the body is specific to each location. For instance, metals are used as biomaterials because of their excellent mechanical properties. Stainless steel, Co-Cr alloys, Titanium alloys, and other metals like platinum, palladium, rhodium, iridium, ruthenium, osmium, and tantalum are examples of the most used metallic biomaterials. The development of modern technology has led to the advancement of manufacturing and fabrication technologies of these biomaterials, which indeed opened the door for an even broader spectrum of biomedical applications.³ One modern approach of metallic biomaterials is a combination of elements to produce multicomponent alloys

which are called high entropy alloys. High entropy alloys are composite materials containing five or more elements in relatively 5–35% concentration to achieve the formation of stable solid alloy solution.⁴ The concept of a high entropy alloy can be found in medical applications such as hip and joint replacements, dental implants, plates, and screws. The high entropy alloys are divided into two main categories to examine their deformation mechanism according to the crystallographic structure of the phase which includes FCC-based, BCC-based, HCP-based, amorphous, and intermetallic high entropy alloys. According to the phase types which include single-phase, dual-phase, eutectic, and multi-phase high entropy alloys (HEAs).⁴ High-entropy alloys are well known for their distinctive microstructural characteristics which gave rise to enhanced properties when compared to conventional alloys. Thermodynamic high entropy effect, lattice distortion effect, sluggish diffusion effect, cocktail effect are the four remarkable properties of high-entropy alloys that assist in determining their solid solution phase, nanostructure, thermal stability, and other important properties. The Thermodynamic high entropy effect is mainly used in explaining the multi-principal-element solid solution. It helps in increasing the formation of the solution phase, with good strength and ductility which make the solution stiffer and better. The lattice distortion describes

*Author for Correspondence: san.balivada@gmail.com

the high strength of HEAs, specifically the BCC-structured HEAs, along with tensile brittleness and slower kinetics. The sluggish diffusion effect explains the nano-sized precipitation. It is mainly used in the casting process. The Cocktail effect is related to the mixing of multicomponent elements of HEA.⁵ When compared to intermetallic compounds that achieve equilibrium states at high temperatures, the high mixing entropy is a multi-principal-element that displays less Gibbs free energy for irregular and partially ordered solid solutions. There is a highly significant difference in the enthalpy observed while mixing dissimilar atomic pairs, which gives rise to the formation of more than two phases. The atomic size difference parameter (δ) also plays an important role in the preparation of high entropy alloys and it is compared with the entropy of mixing (ΔS_{mix}) as well as enthalpy of mixing (ΔH_{mix}) which also explains setting phase selection rule and the order-disorder contesting in these alloys.⁶ While designing any alloy, previous research focused mostly on the corners of a phase diagram to develop conventional alloy which usually occupies only a small portion of the design space. There are many strategies towards the designing approach that assist in shifting the focus towards the central portion of the design space.

PROPERTIES TO DESIGN ALLOYS

Properties such as enthalpy of mixing, the entropy of mixing, melting points, atomic size difference, and valence electron concentration are used in designing high entropy alloys through the phase formation rule. These rules and specifications allow us to design a high-entropy alloy with the specific features that appropriately suit their proposed application.⁶⁻⁸

Enthalpy and Entropy of Mixing

The entropy of mixing of an alloy is similar to that of an ideal gas when the equal atomic size and loose atomic packing are presumed and there is a comparison in the solid-state phases of an alloy, those are elemental phases, intermetallic compound phases, and solid solution phases (random/irregular solid solutions and partially ordered solid solutions).⁶ The phase with very little free energy at a given temperature and pressure will be prevailing in the equilibrium state. If kinetic factors are not included in it, then phase formation is thermodynamically controlled by the Gibbs free energy,

$$\Delta G_{mix} = \Delta H_{mix} - T \times \Delta S_{mix}$$

(where, ΔH = enthalpy of mixing, ΔS_{mix} = entropy of mixing, T = temperature)^{6,7}

Ω Parameter

It gives the integrated effects of ΔS_{mix} and ΔH_{mix} on the stability of different components of solid solution, by taking these various components melting points into the discussion. The Ω and T_m specifications are defined by $\Omega = T_m \cdot \Delta S_{mix} / |\Delta H_{mix}|$.^{6,7}

Where, $\Delta S_{mix} > 1.6R$ (R = gas constant) as a standard for high-entropy alloys, many researchers proposed if $\Omega > 1.1$, where higher the Ω value, the higher the chances of making a single-phase random solid solution in high-entropy alloy

Atomic Size Difference

The critical atomic size difference (δ) found for a solid solution to form high-entropy alloys is $\delta \leq 6.6\%$.^{6,7}

Φ parameter

The individual parameters SC and SE with T_m and ΔH_{mix} , give rise to the ϕ parameter, which defined as

$$\Phi = SC |\Delta H_{mix}| = T_m / |SE|$$

(where, SC is equivalent to ΔS_{mix} , SE = function of atomic composition).^{6,7}

Both ΔS_{mix} and Ω had remarkable expressions in their specific values introduced for the high-entropy alloys with various kinds of phases, and ϕ has shown to be good out of all other three specifications which discussed earlier, with a critical value of $\Phi_c = 20$, where alloys with greater values of Φ_c shows single-phase solid solutions, and lower values show multiphase and amorphous solutions.

Valence Electron Concentration

The valence electron concentration (VEC) shows the type of structure that will be making high-entropy alloys, which are usually face-centered cubic (FCC), body-centered cubic BCC, or hexagonal close-packed (HCP) structures (6). The valence electron concentration, which directs the crystal structure of HEA, is involved in their creation. VEC (6.87) = BCC structure, (>8) = FCC structure, (3) = HCP structure are the stable electron concentrations (Figures 1 and 2).^{6,7}

MATERIALS AND METHODS

There are many methods for preparing HEA that include Powder metallurgy where we prepare the alloying step by step

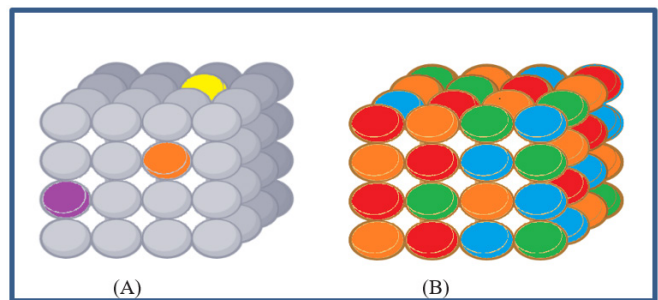


Figure 1: (A) conventional Alloys (B) High Entropy Alloys

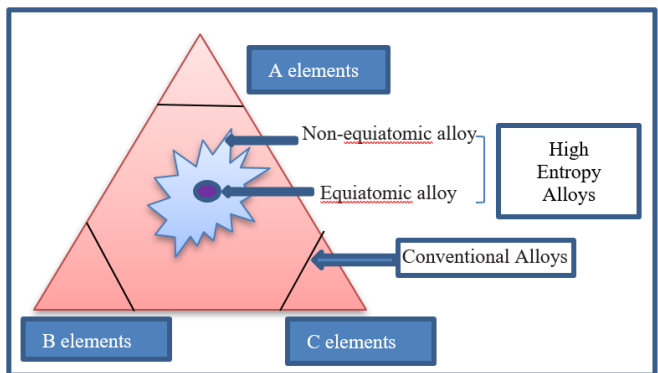


Figure 2: Ternary phase diagram of High Entropy and Conventional Alloys

using ball milling/mixing, pressing, sintering, and subsequent processing. The surface of the substrate is clad with the alloy powder on the substrate in Laser cladding. Separate metal atoms off the surface of the target using direct current or radiofrequency in magnetron sputtering. Most HEA is prepared in bulk using ingot metallurgy, powder metallurgy, and selective laser melting techniques. However, laser cladding and magnetron sputtering methods are mostly used for synthesizing thin films or coatings of HEA.

TITANIUM-BASED ALLOYS

In recent years, many HEAs are used as medical implants, consisting of refractory elements with non-toxic and non-allergenic nature. Many of these alloys have desirable properties for biomedical applications, among which Titanium-based alloys show remarkable biocompatibility with low young modulus, good wear resistance, corrosion resistance, and low magnetic susceptibility.

Ti-Ta-Zr-Hf-Nb

Metallic biomaterials like 316L, Co-Cr-Mo and Ti-6Al-4V show low biocompatibility besides poor wear and corrosion resistance. To overcome this situation the concept of refractory high entropy alloy was introduced to synthesize novel biomaterials like -Ta-Zr-Hf-Nb and $Ti_{1.5}ZrTa_{0.5}Hf_{0.5}Nb_{0.5}$ exhibit superior wear resistance, wettability, corrosion resistance. Where the Ti-Ta-Zr-Hf-Nb system constitutes non-toxic, allergy-free, low young modulus, and low magnetic susceptibility. Ti-Ta-Zr-Hf-Nb is synthesized by Arc meting (Mixture of pure metal in Titanium getter high purity Argon atm.) and vacuum arc melting; Ti-Ta-Hf-Nb-Zr films are deposited by Radio Frequency magnetron sputtering (argon

ions are accelerated by Radiofrequency electric field to hit a target made of the material to sputter) over Ti-6Al-4V substrates. Ti-6Al-4V shows less biocompatibility which is improved by deposition of Ti-Ta-Zr-Hf-Nb on it.

Mechanical properties of the alloys change rapidly when the alloy composition changes. Young modulus is one of the intrinsic natures of materials and its crystalline structure has a dramatic effect on its value. Alloy 1, 2, 3, 4, 5, 6 shows BCC structure having lower young modulus and high yield strength since BCC phase shows low young modulus than HCP Phase. On comparing (alloy 6) with $Ti_{1.5}ZrTa_{0.5}Hf_{0.5}Nb_{0.5}$, the young modulus decreases, and strength increases as the composition is altered. Upon comparing equimolar $Ti_{20}Zr_{20}Hf_{20}Nb_{20}Ta_{20}$ with $Ti_{31.6}Zr_{31.6}Nb_{31.66}Ta_5$ (Alloy 2) it is evident that high young modulus also has high yield strength thereupon it leads to an increase in corrosion resistance. Compared to the bulk form of Ti-Ta-Hf-Nb-Zr, Ti-6Al-4V films show the increasing mechanical property in terms of young modulus (Table 1).⁹⁻¹³

Multi-principal-element (Ti-Zr-Nb-Hf-Ta) N [N= nitrides] and (Ti-Zr-Nb-Hf-Ta) C [C= carbide] protection coatings are be done by DC magnetron sputtering for biomedical applications. The (Ti-Zr-Nb-Hf-Ta) N film has a quasi-stoichiometric composition. However, the (Ti-Zr-Nb-Hf-Ta) C-1 and (Ti-Zr-Nb-Hf-Ta) C2 films are sub-stoichiometric; over stoichiometric respectively, there are remarkable differences between the (Ti-Zr-Nb-Hf-Ta) C-1 and (Ti-Zr-Nb-Hf-Ta) C-2 coatings. For the over-stoichiometric films, metal-containing carbon shows the presence of C-C bonds, and for the sub-stoichiometric film, C-C bonds were not detected. Carbide coating with the highest carbon content shows the best friction performance ($\mu = 0.12$) and the highest wear resistance in the tribological tests

Table 1: Comparison of mechanical properties between various titanium-based alloys

| Ref | Composite & concentration materials | Composite preparation technique | Youngs Modulus (Gpa) | Yield strength (MPa) |
|------|---|--|----------------------|----------------------|
| (9) | $Ti_{25}Zr_{25}Nb_{25}Ta_{25}$ (Alloy1) | Arc meting (Mixture of pure metal in Ti getter high purity Argon atm.) | 89 | 970 |
| (9) | $Ti_{31.6}Zr_{31.6}Nb_{31.66}Ta_5$ (Alloy 2) | Arc meting | 75 | 790 |
| (9) | $Ti_{35}Zr_{35}Nb_{25}Ta_5$ (Alloy 3) | Arc meting | 69 | 780 |
| (9) | $Ti_{45}Zr_{45}Nb_5Ta_5$ (Alloy 4) | Arc meting | 57 | 690 |
| (9) | $Ti_{21.67}Zr_{21.67}Nb_{21.66}Ta_{35}$ (Alloy 5) | Arc meting | 93 | 1050 |
| (9) | $Ti_{15}Zr_{15}Nb_{35}Ta_{35}$ (alloy 6) | Arc meting | 135 | 970 |
| (11) | $Ti_{1.5}ZrTa_{0.5}Hf_{0.5}Nb_{0.5}$ | Arc meting | 98.57 ± 4.18 | 800–1500 |
| (10) | $Ti_{20}Zr_{20}Hf_{20}Nb_{20}Ta_{20}$ | Arc meting | 80 | 800–985 |
| (12) | TiTaHfNbZr filmsTi-6Al-4V substrates | RF magnetron sputtering | 181.3 ± 2.4 | - |
| (13) | TaNbHfZrTi | Vacuum arc melting | 131.6 | - |

Table 2: Comparison of tribological properties between various titanium-based alloys

| Ref | Composite and concentration Material | Coefficient of friction | Wear rate (10^{-4}) mm ³ /Nm |
|------|--------------------------------------|-------------------------|---|
| (12) | Ta-Nb-Hf-Zr-Ti HEA film | 0.1 to 0.2 | $0.5-1 \times 10^{-6}$ mm ³ N-1m-1 |
| (13) | (Ti-Zr-Nb-Hf-Ta) C-1 coating | 0.32 | 0.90×10^{-6} mm ³ N-1m-1 |
| (13) | (Ti-Zr-Nb-Hf-Ta) N coating | 0.17 | 0.29×10^{-6} mm ³ N-1m-1 |
| (13) | (Ti-Zr-Nb-Hf-Ta) C-2 coating | 0.12 | 0.20×10^{-6} mm ³ N-1m-1 |

performed in simulated body fluids (SBFs). The Coefficient of friction is low and stable with the value ranging from 0.1 to 0.2 for TaNbHfZrTi HEA film (Table 2).^{12,13}

Speaking of its biocompatibility, the cell adhesion to substrates is used in assessing cell surface interactions there upon evaluating its biocompatibility according to the literature. X-ray photoelectron spectroscopy (XPS) analysis gives the idea about the formation of a passive film composed of TiO₂, ZrO₂, HfO₂, Nb₂O₅, and Ta₂O₅ which is responsible for high bio-corrosion resistance of high entropy alloy, good adhesion, cell viability, cell proliferation behaviors of MC3T3-E1 pre-osteoblasts on the Ti-Zr-Hf-Nb-Ta HEA indicating well in In-vitro biocompatibility. Ti-Zr-Hf-Nb-Ta HEA is composed of five biocompatible elements Ti, Zr, Hf, Nb, Ta, which shows non-cytotoxic surface film character and high corrosion resistance, less release of corrosion products or ions during in-vivo implantation. Ti-Ta-Hf-Nb-Zr high entropy alloys are used in fetal bovine serum to assess their biocompatibility in presence of proteins so it has the potential to be used in orthopedic implant materials.¹⁴

Ti-Ta-Mo-Nb-Zr

A novel Ti-Ta-Nb-Mo-Zr composite is obtained from an equiatomic Ti-Ta-Nb-Zr alloy which is synthesized from arc melting. There are different types of composites of the Ti-Ta-Nb-Mo-Zr i.e., Ti_{2.6}NbTaZrMo, Ti_{1.7}NbTaZrMo_{0.5}, Ti_{1.5}NbTaZrMo_{0.5}, Ti_{1.4}Nb_{0.6}Ta_{0.6}Zr_{1.4}Mo_{0.6} that show excellent biocompatibility. Among these composites, Ti_{1.4}Nb_{0.6}Ta_{0.6}Zr_{1.4}Mo_{0.6} which is obtained by electrode induction melting gas has decreased melting point and enhanced ductility; its atomization of pre-alloyed rods. Mechanical properties like young modulus and hardness are evaluated using nano-indentation tests. However, stress, strain, and yield strength are obtained by a universal testing machine.

Ti-Ta-Nb-Mo-Zr alloy shows a lower young modulus and yield strength when compared to BCC1 phase alloy. As-cast Ti-Ta-Nb-Mo-Zr alloy consists of two phases BCC1 and BCC2 which are prepared by arc melting, the BCC1 phase shows

high young modulus and yield strength than the BCC2 phase which means the BCC1 phase is harder and stiffer than the BCC2 phase. However, decreasing in young modulus and a decrease in yield strength observe in Ti_{1.4}Nb_{0.6}Ta_{0.6}Zr_{1.4}Mo_{0.6} compared to Ti-Ta-Nb-Mo-Zr alloy. The Selective laser melting rapid solidification feature is successful in imparting excellent mechanical properties to Ti_{1.4}Nb_{0.6}Ta_{0.6}Zr_{1.4}Mo_{0.6} alloy (Table 3).¹⁵⁻¹⁸

HEA under both dry and wet sliding conditions. The dry and wet wear rates of Ti-Zr-Nb-Ta-Mo are lower than Ti-6Al-4V which is 3.5*10⁻⁷ mm³mm⁻¹N⁻¹ and 4.6*10⁻⁷ mm³mm⁻¹N⁻¹. Ti_{0.5}ZrNbTaMo shows a lower coefficient of friction and wear rate in both dry and wet conditions than TiZrNbTaMo alloy. Coefficient of friction and wear rate decrease when they are under wet sliding conditions (Table 4).^{19,20}

Speaking of Biocompatibility, SLM-built Ti_{1.4}Nb_{0.6}Ta_{0.6}Zr_{1.4}Mo_{0.6} with as-cast counterparts, commercially Pure Titanium, and SS316L all show osteoblast density adhered to the specimens when they were evaluated using Giemsa staining. The cell adhesion and proliferation behavior of MC3T3-E1 osteoblast on the surface of the equiatomic ratio of TaNbHfZrTi are not significantly different from Ti-6Al-4V alloy, indicating good biocompatibility due to high corrosion resistance of Mo than Hf in the body fluid.

Ti-Ta-Fe-Zr-Nb

The Ti-Ta-Fe-Zr-Nb, HEA were investigated for the influence of milling time, mechanical properties, compaction, and sintering. They are synthesized by cold rolling, powder metallurgy, arc melting, and thermal processing. Beta titanium alloys (beta-type Ti-based alloys) are a more flexible class of titanium alloys. They are generally used for manufacturing orthopedic and dental implants, as they show the greatest strength to weight ratios, low young modulus, a better combination of strength, toughness, and fatigue resistance, as compared to alpha+ beta type Ti-alloys. While manufacturing high entropy alloy hard coatings is done by high power

Table 3: Comparison of mechanical properties between various Ti-Ta-Mo-Nb-Zr alloys

| Ref | Composite & concentration materials | Composite preparation technique | Youngs Modulus (Gpa) | Yield strength (MPa) |
|------|---|--------------------------------------|----------------------|----------------------|
| (15) | Ti-Ta-Nb-Mo-Zr | Arc melting | 153 | 1390 |
| (15) | Ti ₁₅ Zr ₁₀ Nb ₂₀ Ta ₃₁ Mo ₂₄ (BCC1) | Arc-melted ingot, XRD for structure | 161 | 2005 |
| (15) | Ti ₂₄ Zr ₄₃ Nb ₁₂ Ta ₈ Mo ₁₃ (BCC2) | Arc-melted ingot, XRD for structure | 133 | 1668 |
| (16) | Ti _{1.4} Nb _{0.6} Ta _{0.6} Zr _{1.4} Mo _{0.6} | Arc melting, selective laser melting | 140 ± 9 | 1140 |

Table 4: Comparison of tribological properties between various Ti-Ta-Mo-Nb-Zr alloys

| Ref | Composite and concentration Material | Coefficient of friction | | Wear-rate (10 ⁻⁴) mm ³ /Nm | |
|------|--------------------------------------|-------------------------|-------|---|---|
| | | Dry | Wet | Dry | Wet |
| (20) | Ti _{0.5} ZrNbTaMo | 0.75 | 0.61, | 2.22* 10 ⁻⁷ mm ³ mm ⁻¹ N-1 | 1.52*10 ⁻⁷ mm ³ mm ⁻¹ N-1 |
| (20) | TiZrNbTaMo | 0.94 | 0.64 | 2.91-3.50*10 ⁻⁷ mm ³ mm ⁻¹ N-1 | 1.85-4.60*10 ⁻⁷ mm ³ mm ⁻¹ N-1 |
| (20) | Ti ₂ ZrNbTaMo | 0.84 | 0.71 | 2.42* 10 ⁻⁷ mm ³ mm ⁻¹ N-1 | 2.45* 10 ⁻⁷ mm ³ mm ⁻¹ N-1 |

impulse magnetron sputtering (HiPIMS) system, in which novel TiZrNbTaFe and TiZrNbTaFeN HEA coatings were produced with an equiatomic TiZrNbTaFe which focused on three different substrates involves 304 stainless steel (ss), 420 SS and P-type Si (100) wafer, using a HiPIMS system at different RN2 ratios. The best biomedical materials used in an orthopedic device with an extended period, need a combination of a low young's modulus, high strength, and approximately matches with the human cortical bone.

Alloys synthesized by powder metallurgy have lower young modulus and higher yield strength, but if they are manufactured using a high-power impulse magnetron sputtering (HiPIMS) system they show high young modulus. So, the milling process is important in synthesizing Ti-Nb-Zr-Ta-Fe alloy. If Ti-Nb-Zr-Ta-Fe alloy is coated with 32% concentration of nitrogen, young modulus increases. This is observed in the case of Ti-Nb-Zr-Fe-O alloy whereas young modulus slightly increases. Different compositions of Ti-Nb-Zr-Fe-O alloy under cold rolling and forged condition shows an increase in young modulus and yield strength compared with solution treatment. The addition of Fe and O into the Ti-Nb-Zr-Fe-O alloy enhances mechanical properties (Table 5).²¹⁻²⁵

Using high power impulses magnetron sputtering system (HiPIMS), one TiZrNbTaFe and three TiZrNbTaFe N coated were manufactured in presence of gas flow ratios (RN2).

TiZrNbTaFe HEA has less coefficient of friction, but a high wear rate. nitrogen coating on TiZrNbTaFe HEA provides a good wear rate as well as coefficient of friction. As coating concentration is high, the wear rate and coefficient of friction are less i.e., having good capacity towards wear and corrosion resistance (Table 6).²⁴

Speaking of biocompatibility, there is a concern related to Fe although all other elements such as Ti, Ta, Nb, Zr show excellent biocompatibility and biological response. Fe is genotoxic and cytotoxic which may be prone to corrosion, so Ti-Ta- Nb-Fe was developed to improve biocompatibility and corrosion resistance properties. Corrosion resistance test is carried out while developing biocompatible HEA with superior characteristics along with an appropriate selection of suitable elements. Confocal micrographs performed on the alloys, along with Ti control, with SOS-2 osteoblast-like cells were observed under seven-day incubation. MTS assays were also performed to show a more quantitative analysis of cell proliferation and survival ability. When the level of confidence is reduced to 90%, the Ti-10Ta-4Fe alloy indicates a slight reduction in cellular response, particularly in comparison to the empty well control; even so, and at this reduced level, such an alloy was distinct from the C.P. Ti control, implying that all examined alloys at least rival existing materials in terms of cellular response.²⁶

Table 5: Comparison of mechanical properties between various alloys of-Ta-Fe-Zr-Nb

| Ref | Composite & concentration materials | Composite preparation technique | Youngs Modulus (Gpa) | Yield strength (Mpa) | Ultimate tensile strength (MPa) |
|------|---|---|----------------------|----------------------|---------------------------------|
| (21) | Ti-Nb-Zr-Ta-Fe | powder metallurgy (PM) route | 52 | 2425 | - |
| (22) | Ti-Nb-Zr-Fe-O | Cold rolling + solution treatment, thermal processing program | 60-107 | - | 903 - 1370 |
| (22) | Ti-20Zr-10Nb-3Ta-1Fe-1O (ST) | solution treatment | 50 | 784 | - |
| (22) | Ti-35.3Nb-5.7Ta-7.3Zr-2Fe-0.4O (forged) | Cold rolling | 107 | 817 | 1130 |
| (24) | Ti-Zr-Nb-Ta-Fe | Powder metallurgy (PM) the route, high power impulse magnetron sputtering (HiPIMS) system | 135± 9 | - | - |
| (24) | TiZrNbTaFe N1 (32.0 at. % nitrogen) | Powder metallurgy (PM) the route, high power impulse magnetron sputtering (HiPIMS) system | 206 ± 2 | - | - |
| (24) | TiZrNbTaFe N3 | Powder metallurgy (PM) the route, high power impulse magnetron sputtering (HiPIMS) system | 265 ± 3 | - | - |

Table 6: Comparison of Tribology properties between various alloys of Ti-Ta-Fe-Nb-Zr

| Ref | Composite and concentration Material | Coefficient of friction | Wear rate (10 ⁻⁴) mm ³ /Nm |
|------|--------------------------------------|-------------------------|---|
| (24) | TiZrNbTaFe | 0.40 ± 0.08 | 9.50 × 10 ⁻⁶ mm ³ N ⁻¹ m ⁻¹ |
| (24) | TiZrNbTaFe N1 | 0.75 ± 0.04 | 3.55 × 10 ⁻⁶ mm ³ N ⁻¹ m ⁻¹ |
| (24) | TiZrNbTaFe N7 | 0.79 ± 0.06 | 1.63 × 10 ⁻⁶ mm ³ N ⁻¹ m ⁻¹ |
| (24) | TiZrNbTaFe N10 | 0.69 ± 0.05 | 2.65 × 10 ⁻⁶ mm ³ N ⁻¹ m ⁻¹ |

ALLOY BASED ON ALUMINUM

In these alloys, aluminum is the most common metal. Aluminum alloys offer high specific strength, excellent casting properties, and a low cost. However, it has low biocompatibility and poor wear and corrosion resistance, making it ineffective for biomedical applications. This can be solved by using micro-arc oxidation (MAO) in the fabrication process, which enhances wear and corrosion resistance. These aluminum-based alloys have been modified for use in orthopedic implants.

Al-Co-Cr-Fe-Ni

The use of multi main elements from diverse elements such as 3d transition elements (Fe, Co, Cr, Cu, Ni) and metals such as Aluminium is one of the novel techniques for the design of HEA. At ambient and cryogenic temperatures, a 3d transition metal derived from a single-based FCC structure exhibits good ductility, high strength, and fracture toughness. At room temperature, the high-strength body-centered-cubic (BCC) AlCoCrFeNi alloy has different structures and characteristics. Transmission and scanning electron microscopy were used to analyze the microstructure of these alloys. With increasing Al content, the crystalline structure changes, and multiple

phase structures arise, ranging from a single face-centered cubic (fcc) structure to a duplex fcc plus body-centered cubic (bcc) structure to a single bcc structure. After that, there's a single bcc structure. Arc melting, powder metallurgy, cold rolling, and spark plasma sintering are used to create the alloy's composition.

It was observed that, (Fe-Co-Ni-Cr-Mn) 100_xAl_x (x = 0–20 at. %), (Al < 8%) and (Fe-Co-Ni-Cr-Mn) 100_xAl_x (x = 0–20 at. %) 8% < Al < 16% alloys yield strength and ultimate tensile strength increases as concentration of aluminum increases. Depending on ductility it shows that, decrease in ultimate strength with an increase in ductility in Al-Co-Cr-Fe-Ni_{2.1} alloy. As compare (Fe-Co-Ni-Cr-Mn) 100_xAl_x with Al_{0.5}Co-Cr-Cu-Fe-Ni (FCC + B2 and σ precipitate) and Al_{0.7}Co-Cr-Fe-Ni (FCC + B2) shows that, a sudden increase in yield strength and ultimate tensile strength in Al_{0.5}CoCrCuFeNi composition. And again, a slight decrease in Al_{0.7}CoCrFeNi alloy as we see the decrease in the composition of alloy with an increase in yield strength and ultimate tensile strength. Equimolar Al₂₅Co₂₅Cr₂₅Fe₂₅ have highest yield strength than Al₄Cr₂₀Co₂₀Fe₂₀Ni₂₀. There is insufficient data about the young modulus of this type of HEA (Table 7).²⁷⁻³²

Table 7: Comparison of mechanical properties between various alloys of Al-Co-Cr-Fe-Ni

| Ref | Composite & concentration materials | Composite preparation technique | Youngs Modulus (Gpa) | Yield strength (Mpa) | Ultimate tensile strength (MPa) |
|------------|--|--|----------------------|----------------------|---------------------------------|
| (27) | (FeCoNiCrMn) 100 _x Al _x (x = 0–20 at. %), (Al < 8%), | arc-melting | - | ~220 | ~ 500 |
| (27) | (FeCoNiCrMn)100 _x Al _x (x = 0–20 at. %) 8% < Al < 16% | arc-melting | - | 832 | 1174 |
| (28) | AlCoCrFeNi _{2.1} (ductility 18 ± 2 %.) | a vacuum induction melting furnace | - | - | 1100 ± 50 MPa |
| (28) | AlCoCrFeNi _{2.1} (ductility 15.4%) | a vacuum induction melting furnace | - | - | 1351 MPa |
| (29), (30) | Al _{0.5} CoCrCuFeNi (FCC + B2 and σ precipitates) | Arc-melted, cast annealed, quenched, cold-rolled | 225.69 | 1284 | 1344 |
| (30) | Al _{0.7} CoCrFeNi (FCC + B2) | Arc-melted, cast annealed, quenched, cold-rolled | | 780 | 1040 |
| | Al ₂₅ Co ₂₅ Cr ₂₅ Fe ₂₅ | powder metallurgy, spark plasma sintering | | 3500 | |
| | Al ₂₀ Cr ₂₀ Co ₂₀ Fe ₂₀ Ni ₂₀ | powder metallurgy, spark plasma sintering | | 2400 | |
| | Al ₁₀ Co ₃₀ Cr ₂₀ Fe ₃₅ Ni ₅ | powder metallurgy, spark plasma sintering | | 1890 | |

Table 8: Comparison of Tribology properties between various alloys of Al-Co-Cr-Fe-Ni

| Ref | Composite and concentration Material | Coefficient of friction | | | | | | Wear rate (10 ⁻⁴) mm ³ /Nm | | | | | |
|------|--|-------------------------|-------|-----------|----------|-------|-----------|--|-------|-----------|----------|-------|-----------|
| | | As- cast | | | nitrided | | | As-cast | | | nitrided | | |
| | | air | water | Acid rain | air | water | Acid rain | air | water | Acid rain | air | water | Acid rain |
| (33) | AlCoCrFeNi | 0.429 | 0.321 | 0.302 | 0.512 | 0.681 | 0.213 | 1.8 | 1.6 | 0.7 | 0.39 | 0.32 | 0.28 |
| (34) | Al ₂₅ Co ₂₅ Cr ₂₅ Fe ₂₅ | - | - | - | - | - | - | 11 × 10 ⁻⁶ (mm ³ /Nm) ± SD 0.3 | | | | | |
| (34) | Al ₂₀ Co ₂₀ Cr ₂₀ Fe ₂₀ Ni ₂₀ | - | - | - | - | - | - | 241 × 10 ⁻⁶ (mm ³ /Nm) ± SD 10 | | | | | |
| (34) | Al ₁₀ Co ₃₀ Cr ₂₀ Fe ₃₅ Ni ₅ | - | - | - | - | - | - | 3.6 × 10 ⁻⁶ (mm ³ /Nm) ± SD 1.1 | | | | | |
| (34) | Al ₁₅ Co ₃₀ Cr ₁₅ Fe ₄₀ Ni ₅ | - | - | - | - | - | - | 0.4 × 10 ⁻⁶ (mm ³ /Nm) ± SD 0.05 | | | | | |

SD: Standard Deviation

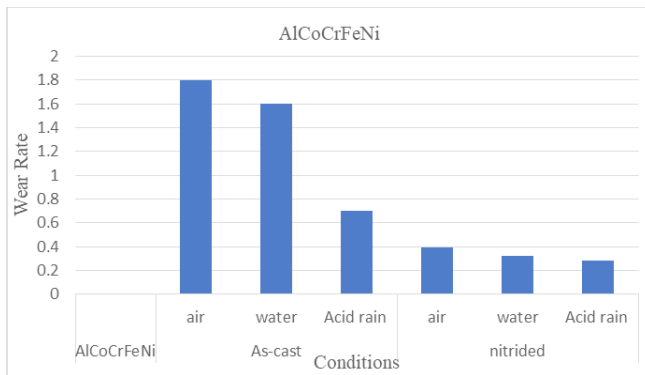


Figure 3: Wear rate of AlCoCrFeNi in different conditions.

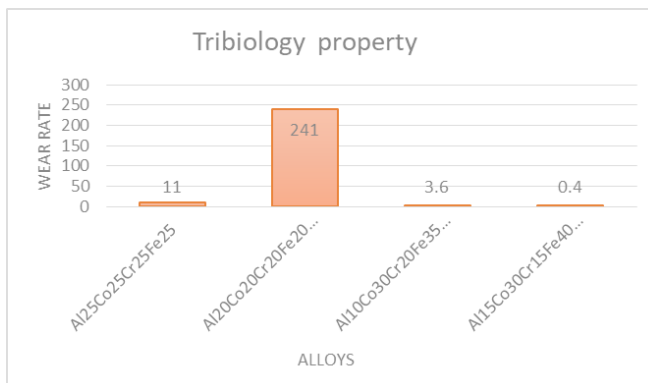


Figure 4: Wear rate of different compositions of Alloys

The plasma nitriding process was used to create a nitrided layer on an AlCoCrFeNi high-entropy alloy. When compared to other alloy compositions. The wear rate of the alloys in deionized water and acid rain was lower than in air, indicating that the lubricating effect of liquid was responsible for the decrease in wear rate and friction coefficient. The friction coefficient of the nitrided alloy in air and deionized water shows higher than that of the as-cast alloy. The tribological characteristics of high entropy alloys with non-equilibrium element concentrations were excellent if compared with equiatomic Al₂₀Co₂₀Cr₂₀Fe₂₀Ni₂₀. And, the non-equilibrium alloys show high hardness and less ductility according to wear rate. And according to the literature, the rate of wear is proportional to the alloy hardness (Figures 3 and 4) (Table 8).^{33,34}

BIOMEDICAL APPLICATIONS

Metallic alloys are used in the preparation of plates, pins, screws, etc. They possess enough rigidity and strength if provided with enough corrosion resistance. Hence, Titanium-based alloys have the potential to perform closest to the cortical bone. They are mainly used for orthopedic devices such as hip joints, bone screws, knee joints, spinal fusion cages, shoulder and elbow joints, and bone plates and scaffolds. It is inert in the human body and can resist attack by body fluids. It is compatible with bone, strong, and has a low young's modulus, higher fatigue strength; that is why it is an outstanding material for orthopedic implants. Most total hip femoral stem, shoulder arthroplasty stems, intramedullary rods are made

of a titanium alloy. When titanium is implanted, it is likely to oxidize. The oxidized titanium coats the implant in a very thin coating of oxidized titanium. This layer has no biological value. Aluminum alloys have a high specific strength, superior casting capabilities, and low cost when compared to Titanium alloys, which are extensively used in bone implants. However, poor wear resistance, corrosion resistance, and insufficient biocompatibility limit their usage in bone replacements.

CONCLUSION

Mechanical properties like Young's modulus, yield strain, and yield stress are measured using a nano-indentation method, where the values change considerably when the composition of the alloy is altered. Especially, Titanium based alloy i.e., Ti-Ta-Zr-Hf-Nb, Ti-Zr-Nb-Ta-Mo, Ti-Zr-Nb-Ta-Fe. Among them, elements like Zr, Nb, Ta have a huge contribution towards corrosion resistance of materials. Equiatomic Ti-Ta-Zr-Hf-Nb alloy with low young modulus 80Gpa, low magnetic susceptibility, yield strength 800-985 Mpa, Ti-Zr-Nb-Ta-Fe it shows low young modulus with high strength but Fe elements having some limitations regarding corrosion resistance. The novel titanium-based alloy shows superior mechanical properties to conventional Titanium alloy. Aluminum-based alloys like Al-Co-Cr-Fe-Ni show better mechanical properties. As the amount of aluminum in the solution increases, the phase shifts from crystalline single FCC to duplex FCC + BCC, and finally to single BCC. However, elements such as aluminum, cobalt, and chromium have limited clinical uses for long-term implant use, and they can cause an immunological response in the human body. As a natural cortical bone, it has a low young modulus and yield strength, which is similar to that of Titanium-based alloys rather than aluminum-based alloys. Finally, as compared to aluminum alloy, the titanium-based alloy has superior mechanical qualities, good biocompatibility, and tribological properties.

DECLARATION OF COMPETING INTEREST

The authors declare that no work in this paper is influenced by any financial interests or personal relationships.

ACKNOWLEDGMENT

We would like to acknowledge the support of the Center of excellence in Additive Manufacturing which is an integral part of the Andhra Pradesh Med Tech Zone (AMTZ) ecosystem and would like to extend our special thanks to MediValley Incubation Center (MVIC) for their constant moral support.

REFERENCES

1. R.E. Smallman, R.J. Bishop, Modern Physical Metallurgy and Materials Engineering (Sixth Edition), Butterworth-Heinemann, 1999; 394-405.
2. Navarro, M., Michiardi, A., Castano, O., & Planell, J. A. Biomaterials in orthopedics. *Journal of the royal society interface*. 2008; 5(27):1137-1158.
3. Zhang, Yong. "History of high-entropy materials." *High-Entropy Materials*. Springer, Singapore. 2019;1-33.
4. Ma, Ning, Shifeng Liu, Wei Liu, Lechun Xie, Daixiu Wei, Liqiang

- Wang, Lanjie Li, Beibei Zhao, and Yan Wang. "Research progress of titanium-based high entropy alloy: methods, properties, and applications." *Frontiers in Bioengineering and Biotechnology* (2020): 1303.
5. Yong Zhang, Ting-Ting Zuo, Zhi Tang, Michael C. Gao, Karin A. Dahmen, Peter K. Liaw, Zhao Ping Lu, Microstructures and properties of high-entropy alloys, *Progress in Materials Science*. 2014; 61:1-93.
 6. Castro, D., Jaeger, P., Baptista, A.C. and Oliveira, J.P., 2021. An overview of high-entropy alloys as biomaterials. *Metals*. 2021;11(4); 648.
 7. Ye, Y. F., Wang, Q., Lu, J., Liu, C. T., & Yang, Y. High-entropy alloy: challenges and prospects. *Materials Today*. 2016;19(6);349-362.
 8. George, E.P., Raabe, D. & Ritchie, R.O. High-entropy alloys. *Nat Rev Mater* 4. 2019; 515–534.
 9. Yuan, Y., Wu, Y., Yang, Z., Liang, X., Lei, Z., Huang, H., Wang, H., Liu, X., An, K., Wu, W. and Lu, Z., Formation, structure, and properties of biocompatible TiZrHfNbTa NbTa high-entropy alloys. *Materials Research Letters*. 2019;7(6):225-231.
 10. Yang, W., Liu, Y., Pang, S., Liaw, P. K., & Zhang, T. Bio-corrosion behavior and in vitro biocompatibility of equimolar TiZrHfNbTa NbTa high-entropy alloy. *Intermetallics*. 2020; 124:106845.
 11. Motallebzadeh, Amir, Naeimeh Sadat Peighambaroust, Saad Sheikh, Hideyuki Murakami, Sheng Guo, and Demircan Canadiens. "Microstructural, mechanical, and electrochemical characterization of TiZrTaHf Nb and Ti1.5ZrTa0.5Hf0.5Nb0.5 refractory high-entropy alloys for biomedical applications." *Intermetallics* 113. 2019; 106572.
 12. N. Tüten, D. Canadiens, A. Motallebzadeh, B. Bal, Microstructure and tribological properties of TiTaHfNbZr high entropy alloy coatings deposited on Ti6Al4V substrates, *Intermetallic*. 2019;105: 99-106.
 13. V. Braic, M. Balaceanu, M. Braic, A. Vladescu, S. Panseri, A. Russo, Characterization of multi-principal- element (TiZrNbHfTa)N and (TiZrNbHfTa)C coatings for biomedical applications, *Journal of the Mechanical Behavior of Biomedical Materials*, 2012;10:197-205.
 14. S. Gurel, A. Nazarahari, D. Canadien, H. Cabuk, B. Bal, Assessment of biocompatibility of novel TiTaHf-based high entropy alloys for utility in orthopedic implants, *Materials Chemistry and Physics*. 2021; 26:124573.
 15. Shao-Ping Wang, Jian Xu, TiZrNbTaMo high-entropy alloy designed for orthopaedic implants: As-cast microstructure and mechanical properties, *Materials Science and Engineering: C*. 2017;73: 80-89.
 16. Takuya Ishimoto, Ryosuke Ozasa, Kana Nakano, Markus Weinmann, Christoph Schnitter, Melanie Stenzel, Aira Matsugaki, Takeshi Nagase, Tadaaki Matsuzaka, Mitsuharu Todai, Hyoung Seop Kim, Takayoshi Nakano, Development of TiNbTaZrMo bio-high entropy alloy (BioHEA) super-solid solution by selective laser melting, and its improved mechanical property and biocompatibility, *Scripta Materialia*. 2021;19: 113658.
 17. Mitsuharu Todai, Takeshi Nagase, Takao Hori, Aira Matsugaki, Aiko Sekita, Takayoshi Nakano, Novel TiNbTaZrMo high-entropy alloys for metallic biomaterials, *Scripta Materialia*, 2017,129; 65-68.
 18. Chien-Chang Juan, Ming-Hung Tsai, Che-Wei Tsai, Chun-Ming Lin, Woei-Ren Wang, Chih-Chao Yang, Swe-Kai Chen, Su-Jien Lin, Jien-Wei Yeh, Enhanced mechanical properties of HfMoTaTiZr and HfMoNbTaTiZr refractory high-entropy alloys, *Intermetallics*. 2015; 62:76-83.
 19. C. Mathiou, A. Pouliou, E. Georgatis, A.E. Karantzalis, Microstructural features and dry - Sliding wear response of MoTaNbZrTi high entropy alloy, *Materials Chemistry and Physics*, 2018; 210: 126-135.
 20. Nengbin Hua, Wenjie Wang, Qianting Wang, Youxiong Ye, Sihan Lin, Lei Zhang, Qiaohang Guo, Jamieson Brechtel, Peter K. Liaw, Mechanical, corrosion, and wear properties of biomedical Ti–Zr–Nb–Ta–Mo high entropy alloys, *Journal of Alloys and Compounds*. 2021; 861:157997
 21. Popescu, G.; Ghiban, B.; A Popescu, C.; Rosu, L.; Trusca, R.; Carcea, I.; Soare, V.; Dumitrescu, D.; Constantin, I.; Olaru, M.T.; et al. New TiZrNbTaFe high entropy alloy used for medical applications. *IOP Conf. Ser. Mater. Sci. Eng.* 2018;400(2): 022049.
 22. Cojocaru, V.D., Nocivin, A., Trisca-Rusu, C., Dan, A., Irimescu, R., Raducanu, D. and Galbinas, B.M. Improving the mechanical properties of a β -type Ti-Nb-Zr-Fe-O Alloy. *Metals*. 2020;10(11):1491.
 23. Ghiban, B., G. Popescu, C. Lazar, L. Rosu, I. Constantin, M. Olaru, and B. Carlan. "Corrosion behavior in human stimulation media of a high entropy titan-based alloy." In *IOP Conference Series: Materials Science and Engineering*. 2018;374(1): 012004.
 24. Sameer Kamrudin Bachani, Chaur-Jeng Wang, Bih-Show Lou, Li-Chun Chang, Jyh-Wei Lee, Fabrication of TiZrNbTaFeN high-entropy alloys coatings by HiPIMS: Effect of nitrogen flow rate on the microstructural development, mechanical and tribological performance, electrical properties and corrosion characteristics, *Journal of Alloys and Compounds*. 2021; 873:159605.
 25. Wang Y, Liu B, Yan K, Wang M, Kabra S, Chiu YL, Dye D, Lee PD, Liu Y, Cai B. Probing deformation mechanisms of a FeCoCrNi high-entropy alloy at 293 and 77 K using in situ neutron diffraction. *Acta Materialia*. 2018; 154:79-89.
 26. Arne Biesiekierski, Jixing Lin, Yuncang Li, Dehai Ping, Yoko Yamabe-Mitarai, Cuie Wen, Investigations into Ti–(Nb, Ta)–Fe alloys for biomedical applications, *Acta Biomaterialia*. 2016;32:336-347.
 27. J.Y. He, W.H. Liu, H. Wang, Y. Wu, X.J. Liu, T.G. Nieh, Z.P. Lu, Effects of Al addition on structural evolution and tensile properties of the FeCoNiCrMn high-entropy alloy system, *Acta Materialia*. 2014; 62:105-113.
 28. Gao, Xuzhou, Yiping Lu, Bo Zhang, Ningning Liang, Guanzhong Wu, Gang Sha, Jizi Liu, and Yonghao Zhao. "Microstructural origins of high strength and high ductility in an AlCoCrFeNi2.1 eutectic high-entropy alloy." *Acta Materialia*. 2017; 141: 59-66.
 29. Weidong Li, Di Xie, Dongyue Li, Yong Zhang, Yanfei Gao, Peter K. Liaw, Mechanical behavior of high-entropy alloys, *Progress in Materials Science*. 2021; 118: 100777.
 30. Jiao, Z.M., Chu, M.Y., Yang, H.J., Wang, Z.H. and Qiao, J.W., Nanoindentation characterised plastic deformation of a Al0.5CoCrFeNi high entropy alloy. *Materials Science and Technology*. 2015;31(10):1244-1249.
 31. Socorro-Perdomo, P.P., Florido-Suárez, N.R., Voiculescu, I. and Mirza-Rosca, J.C., Comparative EIS Study of AlxCoCrFeNi Alloys in Ringer's Solution for Medical Instruments. *Metals*. 2021; 11(6):928.
 32. Liu, J., Guo, X., Lin, Q., He, Z., An, X., Li, L., Liaw, P.K., Liao, X., Yu, L., Lin, J. and Xie, L., Excellent ductility and serration feature of metastable CoCrFeNi high-entropy alloy at extremely

- low temperatures. *Science China Materials*. 2019; 62(6):853-863.
33. Yongxiang Wang, Yaojun Yang, Huijun Yang, Min Zhang, Shengguo Ma, Junwei Qiao, Microstructure and wear properties of nitrided $\text{Al}_x\text{CoCrFeNi}$ high-entropy alloy, *Materials Chemistry and Physics*. 2018; 210: 233-239.
34. Rogal, L., Szklarz, Z., Bobrowski, P., Kalita, D., Garzeł, G., Tarasek, A., Kot, M. and Szlezynger, M., Microstructure and mechanical properties of Al–Co–Cr–Fe–Ni base high entropy alloys obtained using powder metallurgy. *Metals and Materials International*. 2019; 25(4):930-945.